



Probabilistic PGA and Arias Intensity maps of Kyrgyzstan (Central Asia)

K. Abdrakhmatov¹, H.-B. Havenith², D. Delvaux³, D. Jongmans⁴ & P. Trefois³

¹Kyrgyz Institute of Seismology, Bishkek, Kyrgyzstan; ²LGIH, University of Liege, Liege, Belgium; ³Department of Geology, Royal Museum of Central Africa, Tervuren, Belgium; ⁴LIRIGM, University Joseph-Fourier, Grenoble, France

Received 3 August 2001; accepted in revised form 7 May 2002

Key words: Arias Intensity, attenuation, Kyrgyzstan, probabilistic PGA maps, seismicity, seismogenic landslide hazard

Abstract

New probabilistic seismic hazard and Arias Intensity maps have been developed for the territory of the Kyrgyz Republic and bordering regions. Data were mainly taken from the seismic catalogue of Kyrgyzstan and partly from the world seismic catalogue. On the base of seismicity and active tectonics, seismic zones were outlined over the area. For these, Gutenberg-Richter laws were defined using mainly instrumental data, but regarding also historical events. Attenuation of acceleration inside the target area could not be determined experimentally since existing strong motion data are insufficient. Therefore, empirical laws defined for other territories, principally Europe and China, were applied to the present hazard computations. Final maps were calculated with the SEISRISKIII program according to EUROCODE8 criteria, i.e. for a period of 50 years with 90% probability of non-exceedance. For long-term prediction, 100 years maps with 90% probability of non-exceedance have been developed. The procedure used for seismic hazard prediction in terms of PGA (Peak Ground Acceleration) was also applied to Arias intensities in order to be able to define regional seismogenic landslide hazard maps.

Introduction

In the last century, Kyrgyzstan has been affected by a series of seismic disasters, the strongest being the $M_s = 8.2$ Kemin earthquake in 1911 (Bogdanovitch et al., 1914, Delvaux et al., 2001). This earthquake killed several hundreds of people by direct or indirect effects as mudflows or landslides. Recently, the $M_s = 7.3$ Suusamyр earthquake affected the Northern and central Tien Shan mountain regions. About 50 people were killed, most of them by the giant Toluk rock avalanche triggered by the earthquake inside the Southern Suusamyр Range (Ghose et al., 1997).

In the frame of the global seismic hazard program (GSHAP), Ulomov et al. (1999) and Zhang et al. (1999) have studied, among others, seismic hazard of Central Asia. Both groups considered most parts of Kyrgyzstan at the highest risk level, i.e. above 0.48 m/s^2 for a return period of 475 years. Yet, these recent probabilistic seismic hazard maps were cal-

culated for large areas and generally smooth PGA levels throughout this relatively small country (less than 200000 km^2). The aim of the present study is to define probabilistic seismic hazard at regional scale. We will refer to Imanbekov et al. (1999) in the matters of local hazards including site effects concerning the city of Bishkek. Site effect studies have also been undertaken by Havenith et al. (in press). These latter have shown that ground motion can be amplified by a factor of up to 10 over a distance of less than 3 km, even on assumed rock sites. These local scale effects are not included in the general PGA map.

A new approach initiated in this study concerns the computation of a probabilistic Arias Intensity (Arias, 1970) maps. The procedure is the same as for PGA computations but attenuation laws are different. Principally we applied empirical laws by Wilson and Keefer (1985) and Keefer and Wilson (1989), but we tried also to define a theoretical relationship on the basis of accelerograms simulated for various mag-

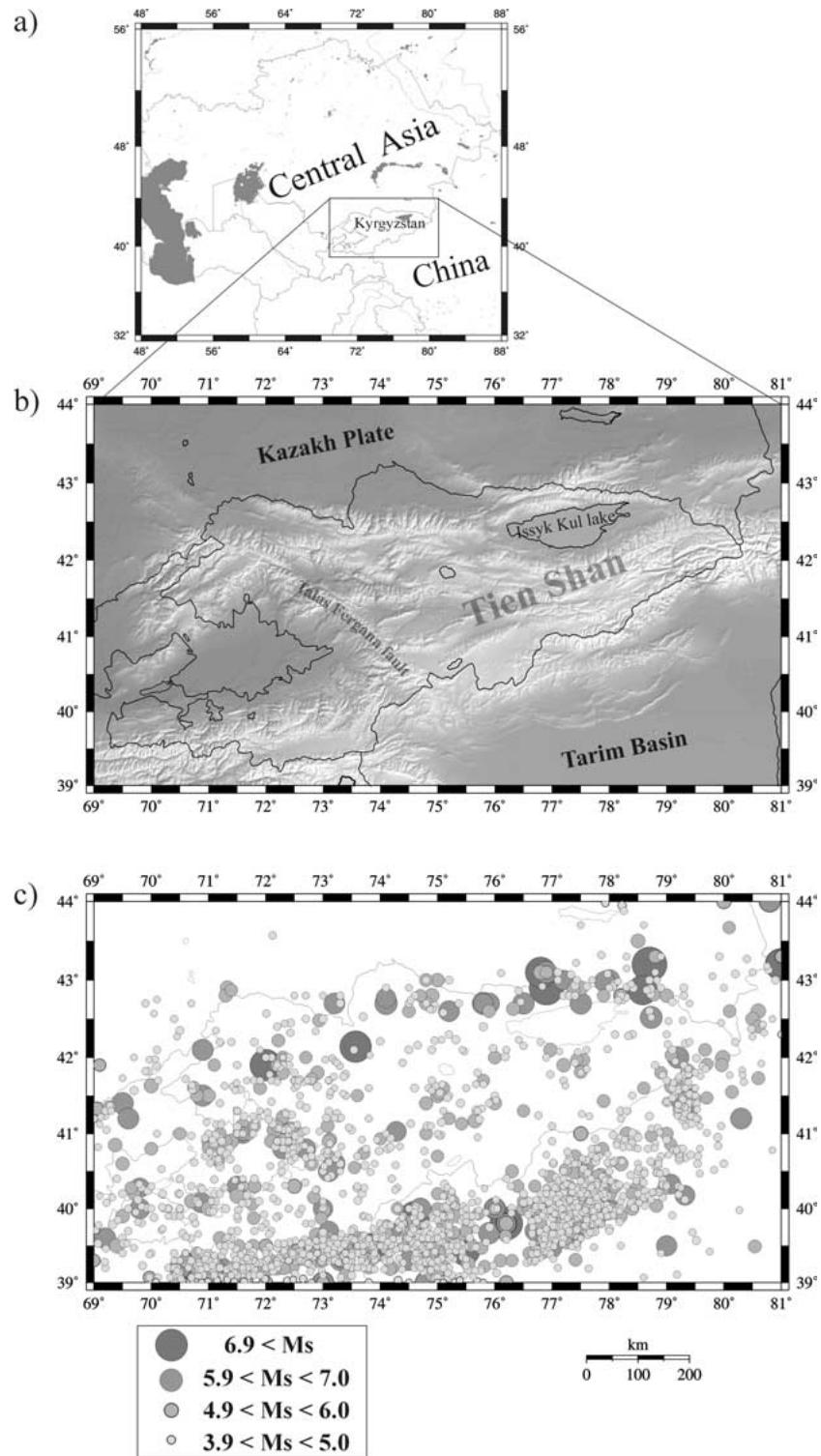


Figure 1. a) Map of Northwestern Central Asia. b) Topographical model of Kyrgyzstan and surrounding regions. c) Historical and instrumental seismicity for the same area.

nitudes and epicentral distances with the stochastic method of Boore (1996).

Geological and tectonic setting

Most of the Kyrgyz territory is occupied by the Tien Shan (Figure 1). This 2500 km long and 500 km broad intracontinental mountain belt consists in a series of E-W trending sub-parallel mountain Ranges (4000–7000 m altitude), separated by intramontane Basins (1000–2000 m altitude). The Tien Shan developed mainly during the Neogene and Quaternary, between the Kazakh platform in the North and the Tarim Basin in the South. After collisional tectonics in the Carboniferous – Permian, tectonic activity resumed in Paleogene times in relation with India-Eurasia collision (Molnar and Tapponnier, 1975; Cobbold et al., 1994). It enhanced in the Miocene, and again at the Pliocene-Quaternary transition (Abdrakhmatov et al., 1996). The stress field during these periods was principally compressive and oriented NS. Present rates of deformation defined by GPS works (Abdrakhmatov, 1996; Reigber et al., 1997) are of the amount of 20 mm per year. This deformation is accompanied by a high seismic activity that affects all of the Tien Shan area (Figure 1c). A particular feature of the Tien Shan is the NW-SE trending Talas Fergana fault (Figure 1b) that accounts for a total dextral displacement of 200 km since Permian times.

Seismic data

Figure 1c shows historical and instrumental seismicity in Kyrgyzstan and bordering regions based on the data of the Kyrgyz (and world) seismic catalogue from 250 BC to 2000. Largest earthquakes in the last 120 years were the Verny (or Alma-Ata, $M_s = 7.3$, 1887), Chilik ($M_s = 8.3$, 1889), Kemin ($M_s = 8.2$, 1911), Chatkal ($M_s = 7.5$, 1946) and Suusamy ($M_s = 7.3$, 1992) earthquakes. These events were generally accompanied by large surface ruptures, such as the Kemin earthquake that activated fault segments with surface rupture over a cumulated length of more than 250 km (Delvaux et al., 2001).

Information about strong earthquakes was collected since 1885, when the Belovodsk event happened (40 km West of Bishkek, $M_s = 6.9$) and was based on macro-seismic observation. In 1927, the first Kyrgyz seismic station was installed at Bishkek (formerly

Frunze). Since then, instrumental data were used to determine earthquake characteristics, precision of epicentre localisation being within 50 km. At the present time, 12 analog and 10 digital stations are working inside the Kyrgyz network; most of them were installed between 1960 and 1970. Precision of epicentre localisation is now estimated at ± 3 km (Muraliev et al., 2000). The Kyrgyz catalogue has been updated till 1996. From then to the present time, i.e. 2001, we completed the database by using events $M_s > 4$ from the world seismic catalogue of the USGS – NEIC (National earthquake Information Centre). The area of request, identical to the area included in the Kyrgyz catalogue, was delimited by 39° and 44° Northern latitude and 69° and 81° Eastern longitude.

Several kinds of problems were encountered by analysing the data: variable magnitude scale or intensity characterisation, changing reliability of indexing with time.

The Kyrgyz seismic catalogue still uses Energetic classes, K (Muraliev et al., 2000), to characterize intensity of events. In the original document, no magnitudes are indicated, and an empirical formula is needed to transform K into M_s (Olga Kuchai, personal communication):

$$K = 4 + 1.8 M_s.$$

This formula was applied to all data. On the other hand, the NEIC catalogue data are characterized by mb for magnitudes lower than 6, while larger magnitudes are defined by M_s or M_w , which are considered as identical. Thus, mb values had to be transformed into M_s to obtain a homogeneous catalogue. Therefore the two catalogues (Kyrgyz and NEIC) were compared for intersecting periods (i.e. between 1973 and 1995) and intersecting magnitudes (i.e. $4 < M_s < 6$). A set of 907 data allowed defining the following empirical relationship:

$$M_s = 1.27 mb - 1.32$$

This formula was then applied to all data of the NEIC catalogue after 31st December 1995. The final compiled catalogue contains about 13000 data ($M_s > 2.9$) since 250BC till 31st December 2000.

Seismic zoning

The complete seismic data set was combined with information concerning tectonics and active faulting in order to define seismic zones over the study area. Figure 2 shows the zoning with regard to topography and

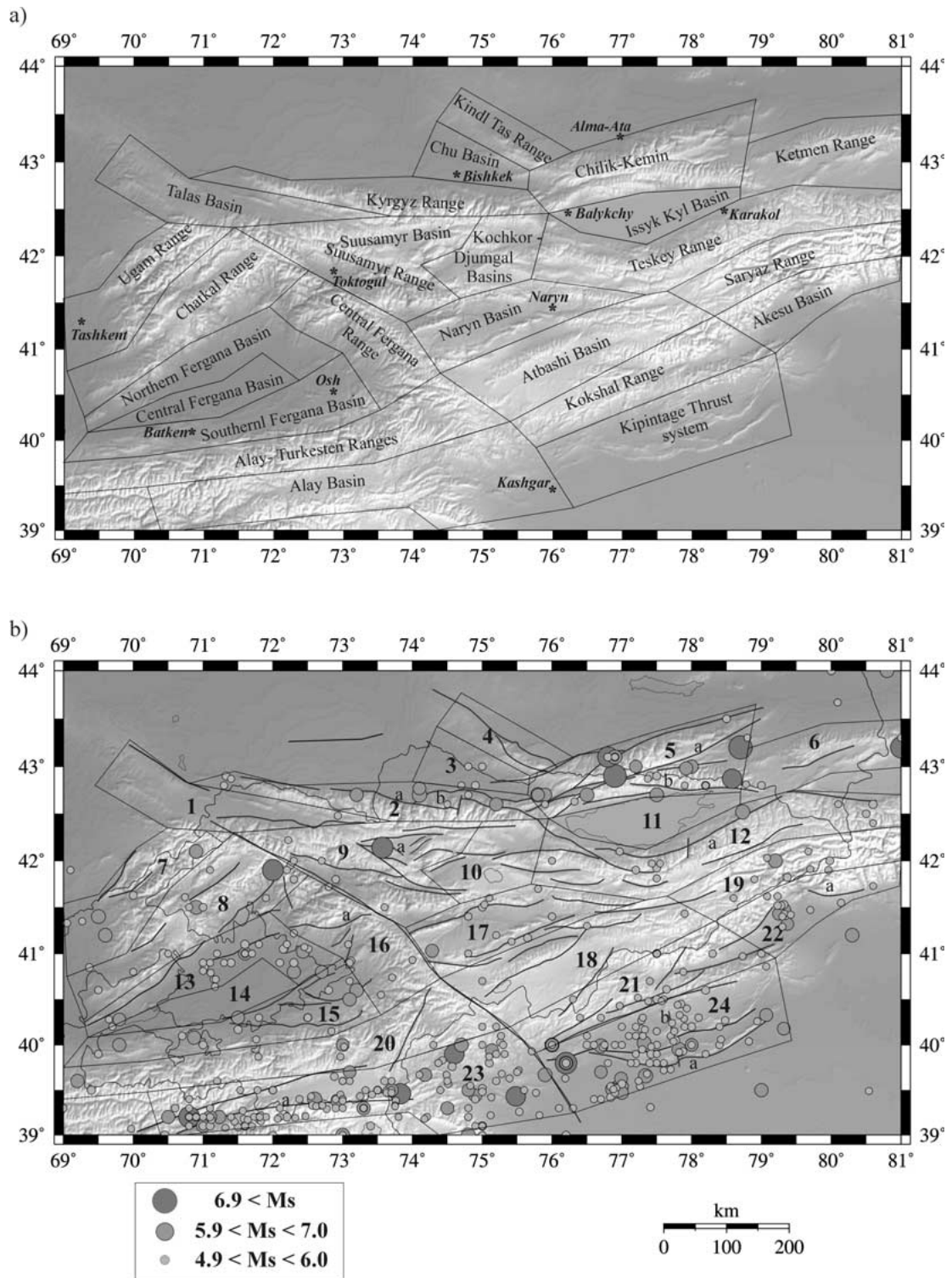


Figure 2. a) Topographical map of Kyrgyzstan and surrounding regions with principal towns and zone names (seismic zones are outlined by bold lines). b) Seismo-tectonic and topographical map with zones indexed from 1 to 24. Zones and several well-known active faults (marked by letters) are referred to in the Annex.

tectonics. The latter information was compiled from Cobbold et al. (1994) for the general structure, from Delvaux et al. (in press) for the Northeastern Tien Shan part, from Allen et al. (1999) for the Southeastern part, from Ghose et al. (1997) for the Suusamyр region and Fan et al. (1994) for the Southern part. Out of all tectonic maps, the main structural feature appeared to be the Talas-Fergana fault. Therefore, the territory was first divided into a Northeastern and Southwestern Tien Shan region to both sides of this fault. During a second step 24 individual zones were outlined according to the Basin-Range structure, which seems to strongly constrain the distribution of seismic activity. A relatively large number of zones were defined in order to highlight local variations of seismicity. Zones are roughly characterized in the Annex.

Gutenberg – Richter laws

In order to calculate reliable Gutenberg-Richter laws for the specific zones, the seismic catalogue was analysed statistically. First we checked if the cumulated number of events does show varying tendencies over time. When analysing the complete set of data, a clear increase of cumulated events appeared between 1927–1930, sharp peaks of activity occurred in 1946, 1949, 1974 and 1992. These four changes can be explained by the large amount of aftershocks related to $M_s = 7.6$ Chatkal event in 1946, the $M_s = 7.4$ Khait event in 1949, the $M_s = 7.3$ Markansu event in 1974 and the $M_s = 7.3$ Suusamyр event in 1992. The aftershock series of these events were subtracted from the catalogue for further treatments. The clear but not sudden increase before 1930 can be linked to the installation of the first seismic station in Bishkek (Frunze) in 1927, because no earthquakes with $M_s < 4$ were indexed before 1927.

Secondly, cumulated events for each Magnitude class were considered separately:

- $3.0 < M_s < 4.1$: beginning in 1929 and increase in 1970. Since 1970, the tendency of cumulated events remains stable till beginning of 1996 (end of catalogue for this class).
- $4.0 < M_s < 5.1$: since 1885 with increase in 1929 and stable behaviour since 1970.
- $5.0 < M_s < 6.1$: since beginning of catalogue with slight increase in 1928 and almost stable slope with a slight decrease between 1955 and 1970.
- $M_s > 6.0$: since beginning of catalogue with no significant change since 1885.

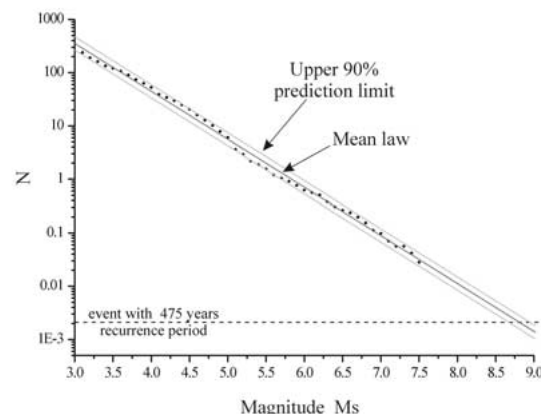


Figure 3. Gutenberg-Richter law and 90%-prediction bands for the entire territory.

According to these results, we decided to exclude the aftershock series of the above-mentioned strong events for Gutenberg-Richter law calculations. In addition, counting was only performed for events of $M_s < 4.1$ between 1970 and 1995, of $4.0 < M_s < 5.1$ between 1970 and 2000 and of $M_s > 5.0$ between 1930 and 2000. For several zones, i.e. Suusamyр and Chatkal regions, Chu Basin Southern Fergana Basin, Saryaz Range and Alay-Turkesten Ranges, the law includes macro-seismic events ($M_s > 5.0$) since 1885. For the two first zones, this procedure allowed us to stabilize the ‘outlier effect’ of the strong Suusamyр and Chatkal events. For the four latter zones, occurrence of significant seismicity was noticed during the period between 1885 and 1930.

Over the whole area between 39° and 44° Northern latitude and 69° and 81° Eastern longitude, the following Gutenberg-Richter law was obtained by fitting the data (Magnitude Range between 3 and 7.6) to the equation $\text{Log}(N) = a - b M_s$ (Figure 3):

$$\text{Log}(N) = 5.25 - 0.9 M_s \quad (1)$$

where N is the number of events per year.

The correlation coefficient R for the log-linear fit is almost -1 . In addition to the mean Gutenberg-Richter law we calculated 90%-prediction bands in order to take into account errors related to the log-linear regression, uncertainties concerning the reliability of the data set or possible variations due to temporal clustering of seismicity.

The upper 90%-prediction limit for the whole area is characterized as follows:

$$\text{Log}(N/\text{yr}) = 5.38 - 0.9 M_s \quad (2)$$

Table 1.

Zone n°	mean law a-value	upper 90%- prediction law a-value	b-value	R	Mmax – mean law 475 years	Mmax – upper prediction law 475 years	Historical Magnitude Mmax
Background	4.00	4.00	0.90	/	7.4	7.4	6.4
Zone 1	2.71	2.94	0.84	-0.97	6.4	6.7	5.3
Zone 2	2.60	2.90	0.75	-0.98	7.0	7.4	6.9
Zone 3	2.06	2.43	0.75	-0.96	6.3	6.8	5.8
Zone 4	2.70	2.90	1.01	-0.96	5.3	5.5	4.3
Zone 5	2.87	3.12	0.70	-0.99	7.9	8.3	8.3
Zone 6	2.78	3.03	0.80	-0.98	6.8	7.1	7.5
Zone 7	2.82	3.01	0.76	-0.99	7.2	7.5	6.7
Zone 8	3.13	3.64	0.80	-0.98	7.3	7.9	7.6
Zone 9	3.33	3.92	0.86	-0.95	7.0	7.7	7.3
Zone 10	2.90	3.11	0.90	-0.97	6.2	6.4	4.9
Zone 11	3.89	4.20	1.30	-0.97	5.1	5.3	4.2
Zone 12	3.22	3.45	0.80	-0.99	7.4	7.7	6.8
Zone 13	4.39	4.59	0.98	-0.99	7.2	7.4	6.4
Zone 14	3.52	4.03	1.00	-0.88	6.2	6.7	5.1
Zone 15	3.64	3.84	0.85	-0.99	7.4	7.7	6.5
Zone 16	4.10	4.47	1.03	-0.97	6.6	6.9	5.5
Zone 17	2.91	3.03	0.79	-1.00	7.1	7.2	6.2
Zone 18	3.44	3.59	1.00	-0.99	6.1	6.3	5.3
Zone 19	3.46	3.74	0.90	-0.99	6.8	7.1	6.7
Zone 20	4.15	4.38	1.01	-0.99	6.8	7.0	6.4
Zone 21	4.09	4.40	0.96	-0.98	7.1	7.4	6.7
Zone 22	4.09	4.28	0.91	-0.99	7.4	7.6	6.6
Zone 23	4.55	4.67	0.85	-1.00	8.5	8.6	7.4
Zone 24	4.44	4.66	0.87	-0.99	8.2	8.4	7.8

For all zones we applied both mean and upper 90%-prediction limit calculations of Gutenberg-Richter laws as shown in Table 1. The b-values are fixed by the linear segment of the data set, but the a-values vary according to the deviations from the linear law. The difference is directly dependent on the correlation coefficient. For most zones, the data were nicely fit by a log-linear law with absolute correlation coefficient higher than 0.95 (Figure 4a, zone 17). For two zones, however, absolute R-values are quite low. This is either due to recent occurrence of very large events (Figure 4b, zone 9 with the $M_s = 7.3$ Suusamyр earthquake) or due to a general misfit of a log-linear law related to a breakdown of the fractal behaviour, partly due to the small number of recorded events (Figure 4c, data of zone 14 showing a poor linear relationship).

For each zone, we calculated the magnitude for a recurrence period of 475 years that can be estimated by both the mean Gutenberg-Richter law and by the upper

90%-prediction limit. The difference between the two is also directly depending on the quality of the fit. The upper estimate of the magnitude is in general much higher than historically observed magnitudes inside a zone. Exceptions are the Kemin-Chilik area where two events (Chilik, Kemin) with magnitudes higher than 8 were recorded and the Ketmen Range where a single large event ($M_s = 7.5$) happened in 1716 at the Eastern limit of the zone.

Attenuation

a) PGA attenuation

Due to the lack of experimental data, no attenuation law is actually known for the Tien Shan. Therefore, we had to apply laws defined for other regions of Eurasia. The first law is the empirical law by Ambraseys et

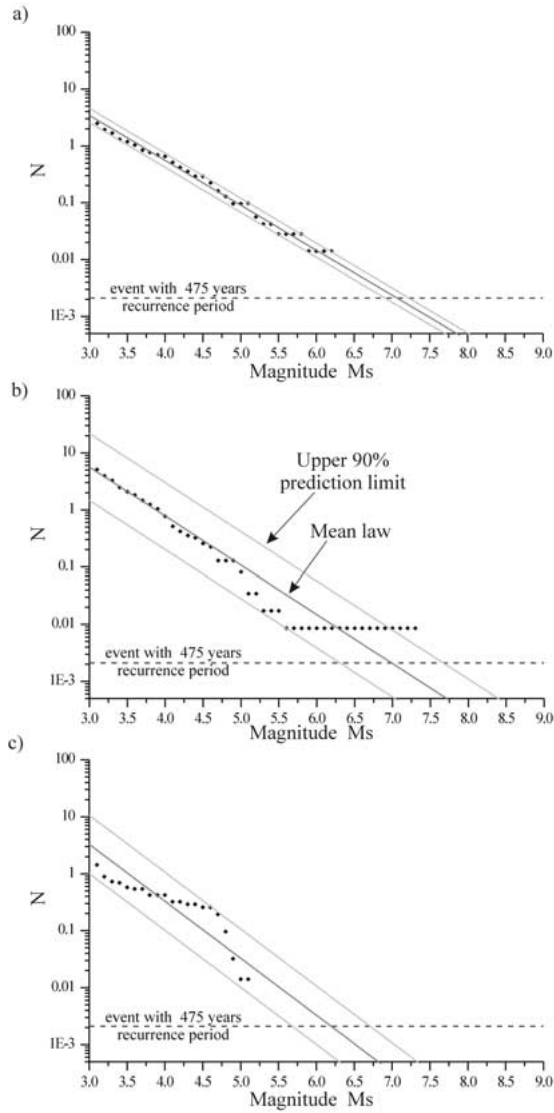


Figure 4. Gutenberg-Richter laws and 90%-prediction bands for three seismic zones: a) Zone17 – Naryn valley – b) Zone 9 – Suisamy region – c) Zone 14 – Central Fergana Basin.

al. (1996), principally based on data from Europe and adjacent regions (extensive, intraplate context).

$$\log a = -1.39 + 0.261 M_s - 0.922 \log r + 0.25 P \quad (3)$$

where a is acceleration in g , r is $\sqrt{d^2 + h_0^2}$ with d the shortest distance to surface projection of the fault rupture and $h_0 = 3.5$. P is 0 for mean values and 1 for 84-percentile values of $\log(a)$. In Figures 5a, 5b and 5c this law is plotted against other laws for three

different magnitudes. To abbreviate this law we will call it hereinafter Am96.

As second law we used the one by Peng et al. (1985) defined for the Yunnan province (Southern China) that shows a Basin and Range structure comparable to the Tien Shan; in the following this law is referred as Pe85:

$$\log a = 0.437 + 0.454 M_s - 0.739 \log R - 0.00279 R \quad (4)$$

where a is acceleration in cm/s^2 , R is the shortest distance to the epicentre. We modified slightly this law to adapt it to the near-field by increasing the R value of the type $\sqrt{R^2 + h^2}$ where h is an arbitrary constant that changes with Magnitude. We fixed the h -value in order to get short distance acceleration values (lower than 20 km^2) similar to the ones of the other attenuation relationships: $h = 15$ for $M_s = 8$, $h = 9$ for $M_s = 7.2$, $h = 6$ for $M_s = 6.4$ and $h = 4$ for $M_s = 5.6$, $M_s = 5.0$ and $M_s = 4.4$ (see Figures 5a, 5b and 5c).

The third law (Huo and Hu, 1992) was applied by Zhang et al. (1999) to the calculation of the seismic hazard map of Continental Asia including our study area. This law (Figures 5a, 5b and 5c), referred afterwards as Hu92, is based on intensity and strong motion data from both China and the Western USA:

$$\ln a = 0.1497 + 1.9088 M_s - 2.049 \ln (R + 0.181 \exp(0.7072 M_s)) \quad (5)$$

where a is acceleration in cm/s^2 , R is the shortest distance to the epicentre.

These two latter laws do not include any standard deviation information. In order to take into account probable uncertainties related with these laws, we added a logarithmic standard deviation of the value of 0.5 (in base e) similar to the one indicated by Am96 of 0.58 (in base e) that corresponds to 0.25P (in base 10) for $P = 1$.

In addition to these empirical laws we computed a theoretical attenuation from simulated accelerograms calculated with the stochastic method by Boore (1996). Stochastic simulation is principally constrained by the source and attenuation parameters. For both parameters, almost no experimental data are available inside the Tien Shan region, besides the stress drop of the Suisamy earthquake estimated by Mellors et al. (1997) to be 17 bars. Therefore, we tried to define commonly applied source and attenuation models. As source we applied the double-corner spectrum model of Joyner (1984) with critical Magnitude of 7 combined with a stress drop of 70 bars,

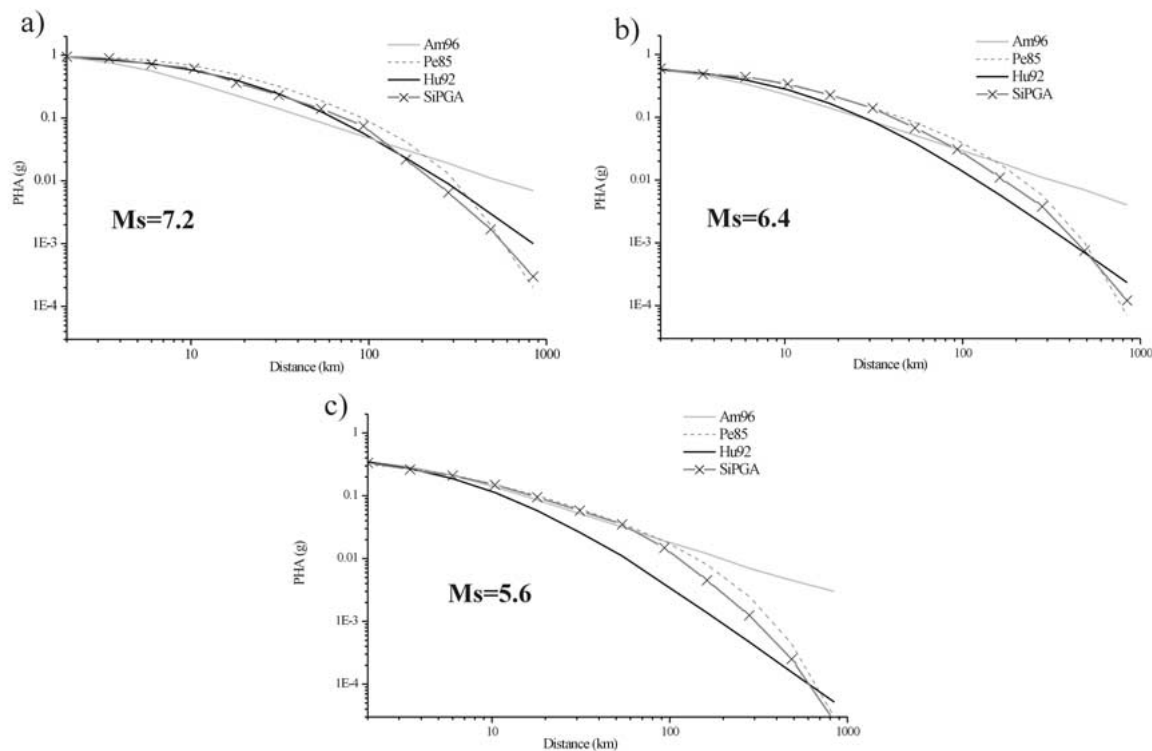


Figure 5. Comparison between four PGA attenuation laws (Ambraseys et al., 1996; Peng et al., 1985; Huo et Hu, 1992; Stochastic simulation) for magnitudes 7.2 (a), 6.4 (b) and 5.6 (c).

which can be considered as a widely accepted value. The high frequency diminution parameter κ was fixed to the usual value of 0.04. As attenuation model we used the one suggested by Atkinson and Silva (1997) for California with $Q = 204 f^{0.56}$. Slight site effects were taken into account by introducing the amplification factors for generic rock sites proposed by Boore and Joyner (1997).

Certainly, the choice of parameter values or of the applied source – attenuation model is almost arbitrary with respect to the large number of models and parameter values available in the literature (Brune, 1970, Atkinson and Boore, 1995, Margaris and Boore, 1998). In fact, we mainly constrained the choice of parameters by comparing the results with the three former attenuation laws. The final model described above produces accelerograms with attenuation characteristics, called hereinafter SiPGA, close to the three empirical relationships (Figures 5a, 5b and 5c).

By comparing all four relationships, it can be seen that the law Am96 shows a stronger attenuation for medium Range distances, but with lowest attenuation

for larger distances. This behaviour is different from the two other experimental laws, which show a higher attenuation for large distances. The simulated attenuation behaviour, SiPGA, presents features comparable to all three former laws but with a closer similarity to law Pe85.

b) Arias Intensity attenuation

The Arias Intensity (Arias, 1970) can be considered as a quantitative measure of the degree of shaking. With respect to the other intensity measures it has the advantage to be more objective and comparable from one earthquake to the other (Harp and Wilson, 1995). The concept has been recently been applied to seismogenic landslide hazard mapping (Jibson et al., 1998; Miles and Ho, 1999). With the same idea we intended to build a probabilistic Arias intensity map for the territory of Kyrgyzstan by applying the same procedure as for PGA mapping but with different attenuation laws.

Arias Intensity is defined as the sum of the energies dissipated per unit weight by a population of oscil-

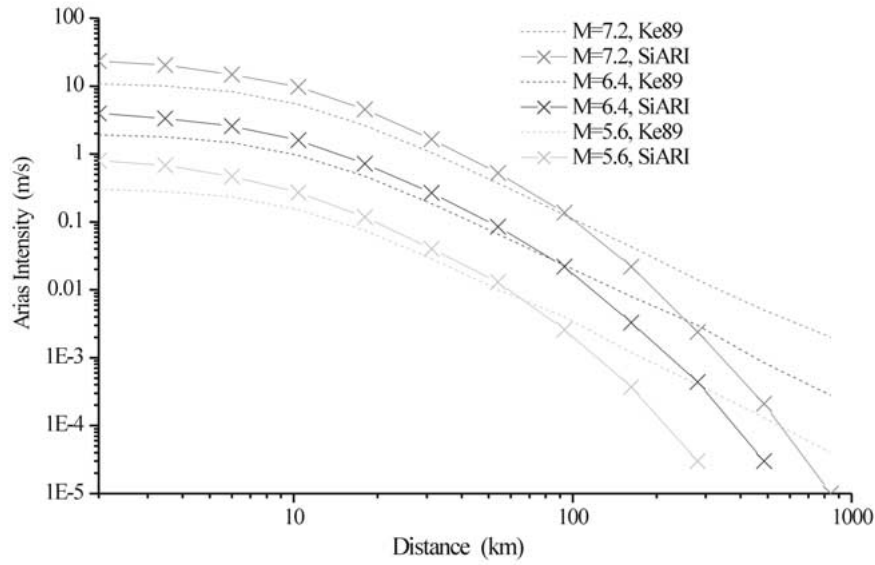


Figure 6. Comparison between two Arias Intensity attenuation laws (Keefe and Wilson, 1985 and 1989; Stochastic simulation) for magnitudes 7.2 (a), 6.4 (b) and 5.6 (c).

lators with resonant frequencies ranging from zero to infinity (Arias, 1970; Harp and Wilson, 1995):

$$I_a = \frac{\pi}{2g} \int_0^{T_d} a(t)^2 dt \quad (6)$$

Wilson and Keefe (1985) were the first to try to correlate seismically triggered landslide distributions with this intensity measure. They also defined the following attenuation relationship in terms of magnitude and distance.

$$\log I_a = -4.1 + M - 2\log R + 0.5P \quad (7)$$

Afterwards, Keefe and Wilson (1989) have reviewed the application of this formula and defined a new one for magnitudes greater than 7.

$$\log I_a = -2.35 + 0.75M - 2\log R \quad (8)$$

We used these two empirical laws, referred afterwards as Ke89, to define Arias intensity attenuation for Kyrgyzstan and included for both a standard deviation of 1.15 corresponding to 0.5 P. In addition, a theoretical intensity attenuation, called SiARI, was defined on the base of the same accelerograms simulated by stochastic method as the ones used for PGA attenuation. For this computed law, we also supposed a standard deviation of 1.15. The comparison

between empirical and theoretical relationships (Figure 6) shows, that by stochastic simulation (SiARI) we obtained higher Intensity values for small epicentral distances but beyond a distance of 60 to 100 km the law Ke89 indicates higher values. The latter can, therefore, be considered as a smoother law.

As comparison we present also an alternative relationship proposed by Faccioli (1995). This attenuation law takes into account source rupture directivity and was calibrated on strong motion data from the Mediterranean region:

$$\log I_a = -4.63 + 1.065M_w - 2\log R + \log D_a(\theta) \quad (9)$$

where R is the hypocentral distance limited within 10 and 50 km. Source directivity is described by the function:

$$D_a(\theta) = \frac{3 - m\cos\theta}{(1 - m\cos\theta)(2 - m\cos\theta)^2} \quad (10)$$

where θ is the angle between the direction of source rupture propagation and the hypocentre-to-receiver direction, m (< 1) is the ratio between rupture propagation and S-wave propagation speeds. The directivity effect is strongest along nearly vertical faults (strike-slip, dip-slip).

Notwithstanding that such a relationship would probably be well adapted to several tectonic regions in

Kyrgyzstan, where strike-slip is predominant, e.g. the Chon Kemin-Chilik zone (Delvaux et al., in press), it can not be easily incorporated in an automatic probabilistic hazard computation scheme. Therefore, only the above-mentioned empirical laws were applied. On the other hand, the anisotropy effect induced by the faults is indirectly taken into account by the outline of the zone generally elongated parallel to the main faults inside this zone.

Probabilistic PGA maps

In the following eight probabilistic PGA maps of Kyrgyzstan are shown, all of them calculated for a 50 years period with 90% probability of non-exceedance. The first four maps (Figure 7a to 7d) are based on mean Gutenberg-Richter law estimates and on the four described attenuation relationships including one standard deviation (0.58 for Am96; 0.5 for the three others). The latter four maps (Figure 8a to 8d) are based on the same attenuation laws and on upper 90%-prediction limit evaluations of the Gutenberg-Richter laws.

By comparing all maps, the ones calculated with Am96 (Figures 7a, 8a) show very smooth PGA variations throughout the area, while strongest changes are computed with Pe85 (Figure 7b, 8b) and Hu92 (Figure 7c, 8c). Over the whole territory, highest PGA values are obtained with Pe85. For high and medium seismic hazard zones, acceleration values computed with SiPGA (Figure 7d) correspond to means between Pe85 and Am96. Due to the smoother far-distance attenuation of Am96, this law involves the relatively highest seismic hazard for bordering regions of the study area, while Hu92 implies a sudden decrease of hazard towards the borders.

Notwithstanding the variations associated with the attenuation laws, a strong dependence on the zoning can be seen on all maps. On the basis of the maps shown in Figure 7, highest seismic hazard principally appears inside three zones: the entire Southern Tien Shan border, the Fergana Basin rim (Southwest) and the Chon Kemin-Chilik region (Northeast).

The general characteristics belong also to the upper 90%-prediction limit estimates with identical attenuation laws, but some high-hazard zones do appear in addition to three above-mentioned ones: the Suusamy, Chatkal and Ugam regions, the Kyrgyz Range and the Teskey Range.

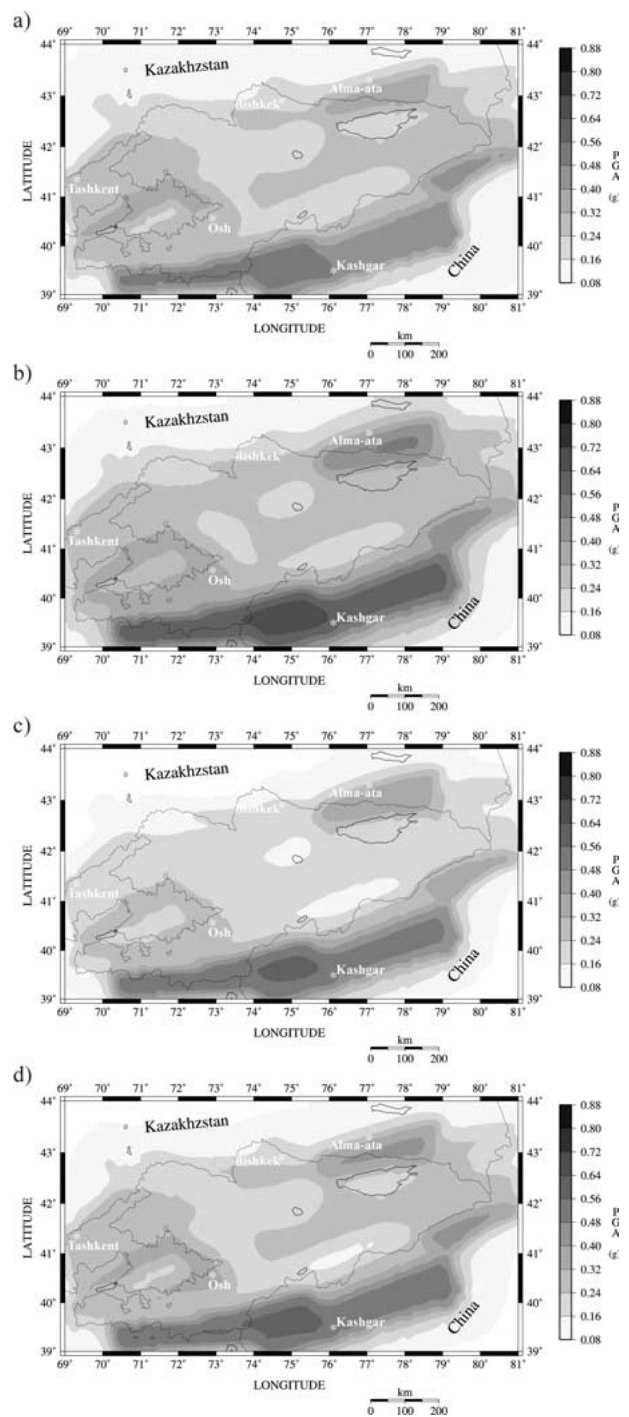


Figure 7. Probabilistic PGA predictions based on mean Gutenberg-Richter law estimates and on 50-year period with 90% probability of non-exceedance. a) PGA map using attenuation relationship by Ambraseys et al., 1996. b) PGA map using attenuation relationship by Peng et al., 1985. c) PGA map using attenuation relationship by Huo et al., 1992. d) PGA map using attenuation relationship determined by stochastic simulation of accelerograms.

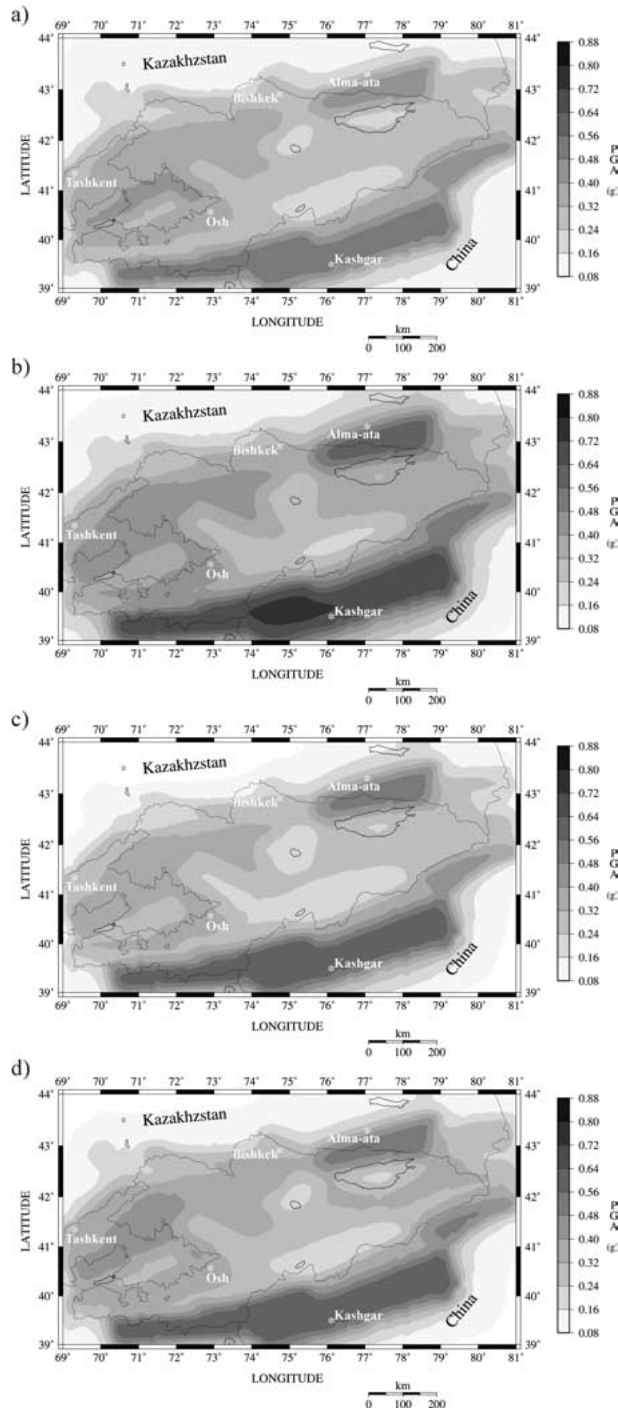


Figure 8. Probabilistic PGA predictions based on upper 90%-prediction limit of Gutenberg-Richter law estimates and on 50 year period with 90% probability of non-exceedance. a) PGA map using attenuation relationship by Ambraseys et al., 1996. b) PGA map using attenuation relationship by Peng et al., 1985. c) PGA map using attenuation relationship by Huo et al., 1992. d) PGA map using attenuation relationship determined by stochastic simulation of accelerograms.

PGA values are still highest along the Southern Tien Shan border with highest values ranging from 0.48–0.56 g (Am96) to more than 0.72–0.80 g (Pe85). The situation for the Chon Kemin-Chilik is also strongly dependant on the attenuation law. Lowest estimates are in the range of 0.4–0.48 g for Am96, highest go up to more than 0.56 g for Pe85. Similar changes are obtained for the Suusamyr region with minimum 0.32–0.40 g for Hu92. Maximum values of 0.4g–0.48g are again shown by the map calculated with Pe85.

Results of seismic hazard prediction for 10 towns in Kyrgyzstan and surrounding regions are displayed in Table 2. For each town, 32 estimates are indicated, corresponding to the modelled cases with Mean and Upper 90% prediction limit laws, the four attenuation relationships (mean and mean plus one standard deviation) and 90% probability of non-exceedance periods of 50 and 100 years. Out of this table, it clearly appears that Kashgar is the town with highest hazard, but Alma-Ata, Osh and Balykchy also show high hazard evaluations.

Actually, for each region and town there are four principal choices of hazard parameters to make: mean or upper prediction G-R law, which one of the four attenuation laws, mean or mean plus one standard deviation attenuation, 50 or 100 year prediction periods?

For the G-R laws, we suggest taking the upper 90% prediction limit laws due to uncertainties of the log-linear fits and also due to possible temporal changes of seismicity that are better taken into account by these upper estimates. The choice of an attenuation model is more difficult since we have no data to constrain it. In this paper we will principally refer to Pe85 since this model produces the highest estimates and therefore the most conservative ones for engineering purposes. For the same reason, the estimates should be based on mean plus one standard deviation attenuation values. Finally, the choice of the prediction period is depending on the engineering project. For example seismic hazards of the Toktogul dam should include all maximum hazard components and this implies a PGA value of 0.5 g for upper prediction G-R, Pe85, and 10% probability of exceedance in 100 years. For this kind of large constructions, a 250-year period with a 10% probability of exceedance may even be more adequate, which implies a maximum PGA of 0.7 g, all other parameters kept identical.

The application of the simulated attenuation relationship or Am96 can be considered as an alternative to the maximum estimates using Pe85, particularly

Table 2.

Towns		Alma-Ata	Balykchy	Batken	Bishkek	Karakol	Kashgar	Naryn	Osh	Tashkent	Toktogul
Longitude		76.95	76.18	70.83	74.60	78.42	76.00	76.00	72.80	69.25	72.83
Latitude		43.25	42.46	40.06	42.87	42.48	39.45	41.42	40.52	41.30	41.80
Mean G-R											
Am96	mean 50	0.16	0.17	0.20	0.15	0.16	0.31	0.17	0.20	0.18	0.15
	mean 100	0.20	0.21	0.25	0.19	0.20	0.37	0.21	0.25	0.22	0.19
	upper 50	0.24	0.26	0.29	0.23	0.25	0.50	0.25	0.30	0.27	0.24
	upper 100	0.32	0.33	0.38	0.29	0.32	0.63	0.33	0.39	0.35	0.30
Pe85	mean 50	0.29	0.29	0.27	0.20	0.24	0.48	0.21	0.27	0.22	0.18
	mean 100	0.39	0.38	0.34	0.26	0.31	0.59	0.27	0.35	0.30	0.24
	upper 50	0.37	0.36	0.35	0.26	0.31	0.64	0.27	0.36	0.29	0.24
	upper 100	0.50	0.49	0.46	0.34	0.41	0.82	0.36	0.47	0.39	0.32
Hu92	mean 50	0.23	0.23	0.23	0.15	0.19	0.42	0.17	0.23	0.19	0.14
	mean 100	0.33	0.32	0.29	0.21	0.26	0.53	0.23	0.30	0.26	0.20
	upper 50	0.28	0.27	0.28	0.19	0.24	0.55	0.21	0.28	0.23	0.17
	upper 100	0.40	0.39	0.38	0.26	0.33	0.71	0.29	0.38	0.33	0.25
SiPGA	mean 50	0.22	0.23	0.24	0.18	0.19	0.40	0.19	0.25	0.21	0.17
	mean 100	0.29	0.30	0.31	0.24	0.24	0.49	0.25	0.32	0.28	0.22
	upper 50	0.30	0.30	0.32	0.24	0.26	0.56	0.25	0.34	0.28	0.23
	upper 100	0.40	0.40	0.41	0.32	0.34	0.70	0.34	0.43	0.36	0.30
Upper pred. G-R											
Am96	mean 50	0.20	0.24	0.23	0.19	0.19	0.33	0.18	0.23	0.20	0.22
	mean 100	0.25	0.30	0.28	0.23	0.23	0.40	0.22	0.28	0.25	0.27
	upper 50	0.31	0.35	0.35	0.30	0.30	0.50	0.28	0.36	0.31	0.34
	upper 100	0.40	0.46	0.45	0.38	0.38	0.64	0.36	0.46	0.40	0.43
Pe85	mean 50	0.37	0.36	0.31	0.26	0.29	0.49	0.23	0.32	0.27	0.30
	mean 100	0.47	0.47	0.39	0.33	0.37	0.60	0.31	0.41	0.35	0.37
	upper 50	0.47	0.46	0.42	0.34	0.38	0.66	0.30	0.43	0.35	0.39
	upper 100	0.63	0.62	0.54	0.45	0.50	0.84	0.40	0.56	0.46	0.50
Hu92	mean 50	0.30	0.30	0.27	0.21	0.24	0.45	0.19	0.27	0.22	0.25
	mean 100	0.41	0.40	0.34	0.28	0.32	0.57	0.26	0.35	0.29	0.32
	upper 50	0.38	0.37	0.34	0.26	0.31	0.61	0.24	0.35	0.27	0.31
	upper 100	0.52	0.51	0.45	0.36	0.41	0.79	0.33	0.46	0.37	0.42
SiPGA	mean 50	0.28	0.29	0.28	0.24	0.23	0.44	0.22	0.29	0.25	0.27
	mean 100	0.36	0.36	0.35	0.30	0.29	0.53	0.28	0.37	0.32	0.34
	upper 50	0.37	0.38	0.37	0.32	0.31	0.61	0.29	0.40	0.33	0.37
	upper 100	0.49	0.50	0.49	0.41	0.41	0.76	0.38	0.51	0.43	0.48

Mean G-R: mean Gutenberg-Richter laws; Upper pred. G-R: upper 90% prediction limit of Gutenberg-Richter law; mean 50: mean attenuation law, for 50-year period; mean100: mean attenuation law, for 100-year period; upper 50: mean attenuation law plus one standard deviation, for 50-year period; upper100: mean attenuation law plus one standard deviation, for 100-year period. Largest estimates of PGA are bold.

for the regions with very large hazards. In fact, the absolute maximum PGA (100 years) for Kashgar of 0.84g might be overestimated, since for these large strains, non-linear effects will appear. Maximum values of 0.76g and 0.64 g calculated with SiPGA and Am96, respectively, seem more probable. However, the application of Am96 might be questionable since this attenuation relationship was determined for an-

other tectonic area, Europe and surrounding regions. The Hu92 law does produce very large PGA values for high hazard regions, but lowest for low or medium hazard regions. Therefore we think that all the models using Hu92 might underestimate hazards in these two kinds of regions.

As we mentioned before, PGA results do not include site effects. This means, that these PGA values

are predicted for rock sites or generic rock sites and it is difficult to predict which kind of situation can be expected in the Fergana valley, the Chu, Naryn, Talas, Issyk Kul, or Suusamyр Basins (among others). On one side, weak or medium ground motions (far field of large earthquakes, near field of small events), will involve large amplifications in these sediment filled Basins; these are most likely to increase the mean level of seismic hazard.

On the other side, for very strong motions it can be expected that non-linear effects, particularly in the near-field on loose sediments, will significantly reduce PGA values. Both, site amplification and non-linear effects will probably tempt to smooth PGA values with regard to earthquakes of different magnitudes and at different epicentral distances. However, site effects certainly change the fundamental frequency of the ground motion. In fact, on loose sediments, amplifications generally affect the low frequency domain (less than 5–10 Hz) and this may have an unfavourable influence on the stability of constructions. To quantify these effects, response spectra must be estimated for the concerned regions, either experimentally, which would be the best way, or theoretically if necessary strong motion data are missing but structural and geotechnical data available. Unfortunately, for this study none of these two approaches could be undertaken due to absence of all kinds of data. Henceforward we will limit our quantitative predictions to rock sites and qualitative estimates to soil sites. In this regard, we refer to Imanbekov et al. (1999) for local amplification effects among the territory of Bishkek and to Havenith et al. (in press) in the matter of surface geology and topographical effects observed in the Northeastern Tien Shan.

Probabilistic Arias Intensity maps

a) Construction of the map

These maps were basically designed in order to be able to predict quantitatively regional hazard of seismogenic landslides in terms of Newmark displacements (Newmark, 1965) using the approach by Jibson et al. (1998). Here, we principally focus on PGA maps and there will be only place for qualitative indications concerning the relationship between Arias Intensity and hazard of seismically triggered landslides.

Keefer and Wilson (1989) defined thresholds of Arias Intensity (Ia) beyond which occurrence of cer-

tain types of slope instability becomes possible. Principally they associated slope instabilities to five groups with the following threshold values of Arias Intensity: type I – with Ia threshold of 0.11 m/s – falls, disrupted slides and avalanches; type II – with Ia threshold of 0.32 m/s – slumps, block slides and earth flows; type III – with Ia threshold of 0.54 m/s – lateral spreads and flows.

The basic parameters of hazard computations are identical to the ones mentioned above, besides the use of different attenuation laws: mean and upper prediction G-R laws, two attenuation laws (Ke89 and SiARI), mean and mean plus one standard deviation attenuation, 50 and 100 year prediction periods.

Out of the different models, we will show the maximum estimates for the two attenuation laws, i.e. including upper prediction G-R law, mean plus one standard deviation attenuation and a 100 prediction period. The two maps projected on the topographical model of the study area are shown in Figures 9a and 9b. Though, SiARI produces slightly higher Arias Intensities, the results can be estimated as similar.

First, by comparing the two maps with Ia threshold values for the different types of landslides, it appears that the whole mountain region is at landslide risk, including all kinds of landslides, since the maximum threshold for lateral spreads of 0.54 m/s is exceeded everywhere. Yet, among the study area, different zones are more at risk than others such as the Southern Tien Shan border, which is clearly outlined as highest hazard zone. But in terms of slope stability hazards, we may constrain the area most at risk to the high mountain slopes North and South of the Alay Basin, the Southern slopes of the Kokshal and Saryaz Ranges and the Kipingtage zone since, there, topography is most accentuated. High Ia values inside the Fergana valley principally imply seismogenic landslide hazard at the Fergana Basin rim. Further, it can be seen that strong Arias Intensities affect the Northwestern and Northern Tien Shan Ranges, such as the Ugam, Chatkal and Pskern (among others) as well as the Kyrgyz and Suusamyр Ranges. In the central Tien Shan (Naryn and Atbashi Ranges), Arias Intensities are generally lower, but still superior to minimum landslide triggering thresholds. The Teskey Range also shows medium Arias Intensity levels. Highest hazard in the Northern Tien Shan, both, in terms of topography and Arias Intensity, affects the Chon Kemin-Chilik region.

Observations made in regions affected by large earthquakes during the last 120 years support the theoretical estimates: rock avalanches in the Kyrgyz

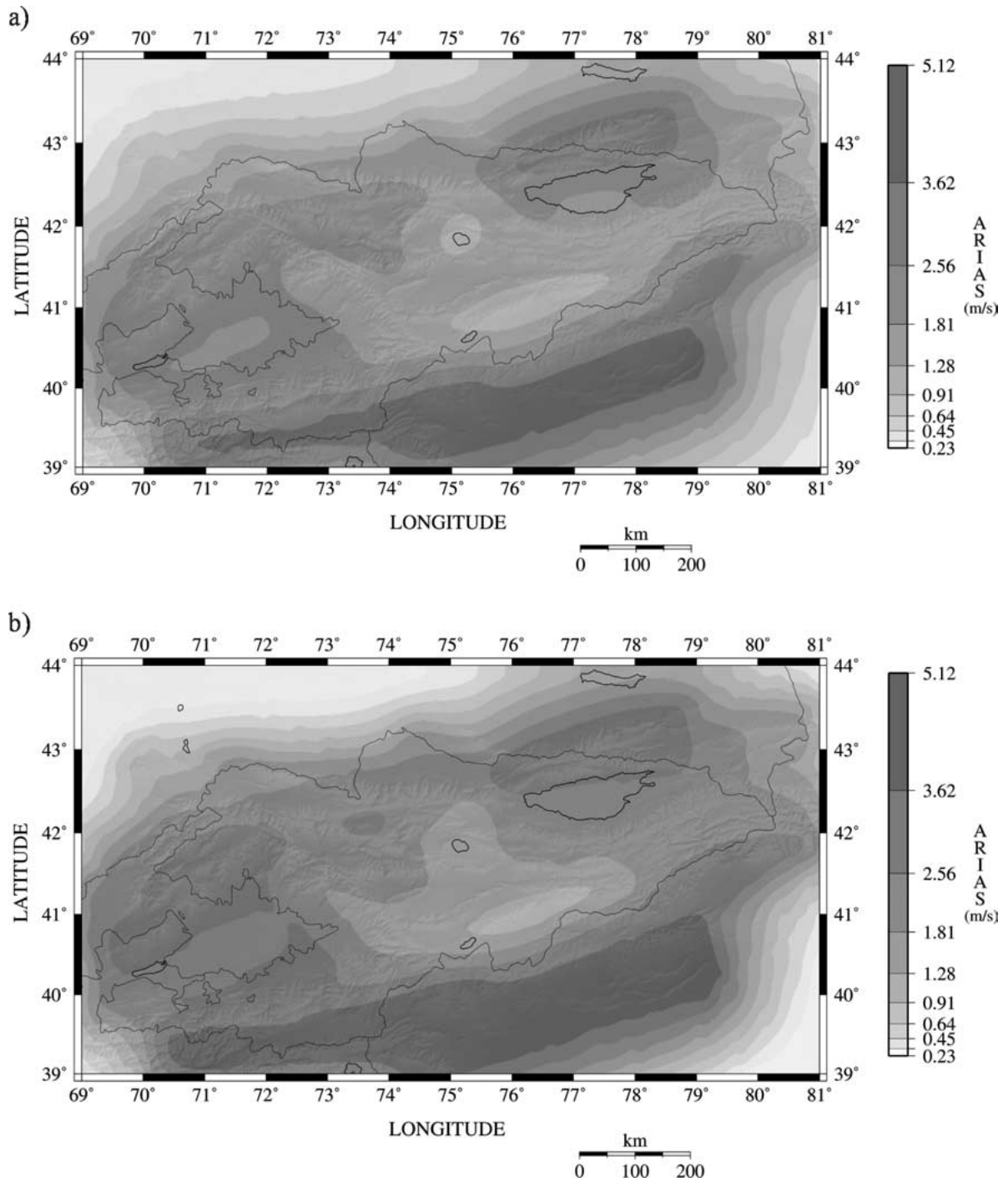


Figure 9. Probabilistic Arias Intensity predictions based on upper 90%-prediction limit of Gutenberg-Richter law estimates and on 100 year period with 90% probability of non-exceedance. a) Arias Intensity map using attenuation relationships by Wilson and Keefer (1985) and Keefer and Wilson (1989). b) Arias Intensity map using attenuation relationship determined by stochastic simulation of accelerograms.

Range triggered by the Belovodsk earthquake in 1885; rock avalanches in the Chon Kemin and Chon Aksu valleys triggered by the Kemin-Chilik earthquake in 1911; debris slumps in the Suusamyр valley and rock avalanches in the Aramsu and Suusamyр Ranges triggered by the Suusamyр earthquake in 1992; slope instabilities regularly triggered in the Mailuu-Suu valley (Northern Fergana Basin).

b) Comparison with existing Intensity maps

In former Soviet Union countries, seismic hazard was generally expressed in terms of 'ballovs'. This scale is an intensity scale and ranges from 0 to 11. Using this scale, Djanuzakov et al. (1995) have built a deterministic seismic hazard map of Kyrgyzstan (Figure 10), principally based on macro-seismic observations. In the following, we try to compare this map with the probabilistic Arias Intensity map using the attenuation law Ke89 and calculated for 100 years.

The map by Djanuzakov et al. (1996) shows three types of ballov-zones: 7-ballovs, 8-ballovs and 9-ballovs zones. Inside the highest seismic hazard zone with 9-ballovs, areas are delimited by hooked lines, where events with magnitudes larger than 7.5 can be expected. Inside the 8-ballovs zone, areas with maximum magnitudes larger than 7.0 are delimited by dashed-hooked lines. The 7-ballovs zone appears only North of Kyrgyzstan.

By comparing this map with our Arias Intensity map using Ke89, similarities and discrepancies can be defined. Most similar are the predictions of large intensities (9 ballovs or $I_a > 1.21$ m/s) in the Chon Kemin-Chilik zone with expected magnitudes larger than 7.5. Large intensities are also predicted by both maps in the Suusamyр, Chatkal and Eastern Fergana Basin regions as well as for the Alay Range and Basin zone. The absence of 9-ball areas in the Central Tien Shan compares with I_a predictions for 100 years lower than 1.21 m/s. Largest differences between the two maps can be outlined for three zones: The ballovs-map predicts large 9-ballovs intensities for the belt along the Talas-Fergana fault as well as for the Eastern Kyrgyz and Teskey Ranges; this does not compare with the medium I_a values (0.91–1.21 m/s) predicted by our map using Ke89. What concerns the Kyrgyz and Teskey Ranges, the difference might be explained by the specificity of the attenuation law, since computations using SiARI do well predict I_a larger than 1.21 m/s for these two zones within 100 years.

The large ballovs-intensity zone along the Talas-Fergana fault among the central Fergana Range still corresponds to a medium I_a zone on the SiARI map. This probably depends on the definition of activity along the Talas-Fergana fault belt. We did not distinguish any significant seismicity (maximum Magnitude of 6.9 expected within 475 years) inside this belt; that is why it appears as a medium-Range Intensity zone on our map. Djanusakov et al. (1995) on the contrary clearly outlined an area along the fault with maximum magnitudes larger than 7.5, which involves larger intensity estimates.

Conclusions

In this paper we applied the technique of probabilistic PGA mapping to the territory of Kyrgyzstan and surrounding regions. The same procedure was also used for defining probabilistic Arias Intensities over the same area. In addition, we introduced the use of stochastic simulation of accelerograms to both probabilistic PGA and intensity mapping. In both cases, results were satisfactory and comparable with those based on experimental attenuation relationships (PGA attenuation: Ambraseys et al., 1996; Peng et al., 1985 and Zhang et al., 1999; Arias intensity attenuation: Wilson and Keefer, 1985; Keefer and Wilson, 1989). The application of stochastic simulation appears interesting if no sufficient strong motion data are available to build an attenuation law. Yet, data of a small number of earthquakes allow the definition of the principal source and attenuation characteristics, which could unfortunately not be done in this study due to the lack of any data.

In order to include uncertainties affecting the Gutenberg-Richter laws of single zones, we took into account the upper 90%-prediction limit of the log-linear fit.

Highest probabilistic PGA were obtained with Peng et al. (1985) whose law has been established in a similar tectonic context, combined with upper 90%-prediction estimates of seismicity.

Both PGA and Arias intensity mapping implied that largest hazards are expected along the Southern Tien Shan border, around the Fergana Basin, among the Chatkal, Ugam and Suusamyр Ranges as well as in the Kemin-Chilik region. Seismic hazards computed for specific large towns indicate that Kashgar and Alma-Ata are most at risk with maximum predictions of 0.66 g and 0.47 g, respectively, for a period

КАРТА СЕЙСМИЧЕСКОГО РАЙОНИРОВАНИЯ ТЕРРИТОРИИ КЫРГЫЗСКОЙ РЕСПУБЛИКИ
 Масштаб 1:1000 000
 1995 г.

Составили: К. Д. Джанузакоев, О. К. Чедия, К. Е. Абдрахматов, А. Т. Турдукулов
 при участии: И. Н. Лемзина, К. Н. Нурманбетова, А. Г. Фролова, Т. М. Саитовой, Е. В. Мураенко, Н. Х. Багмановой, К. А. Садыковой, Т. А. Чаримова.

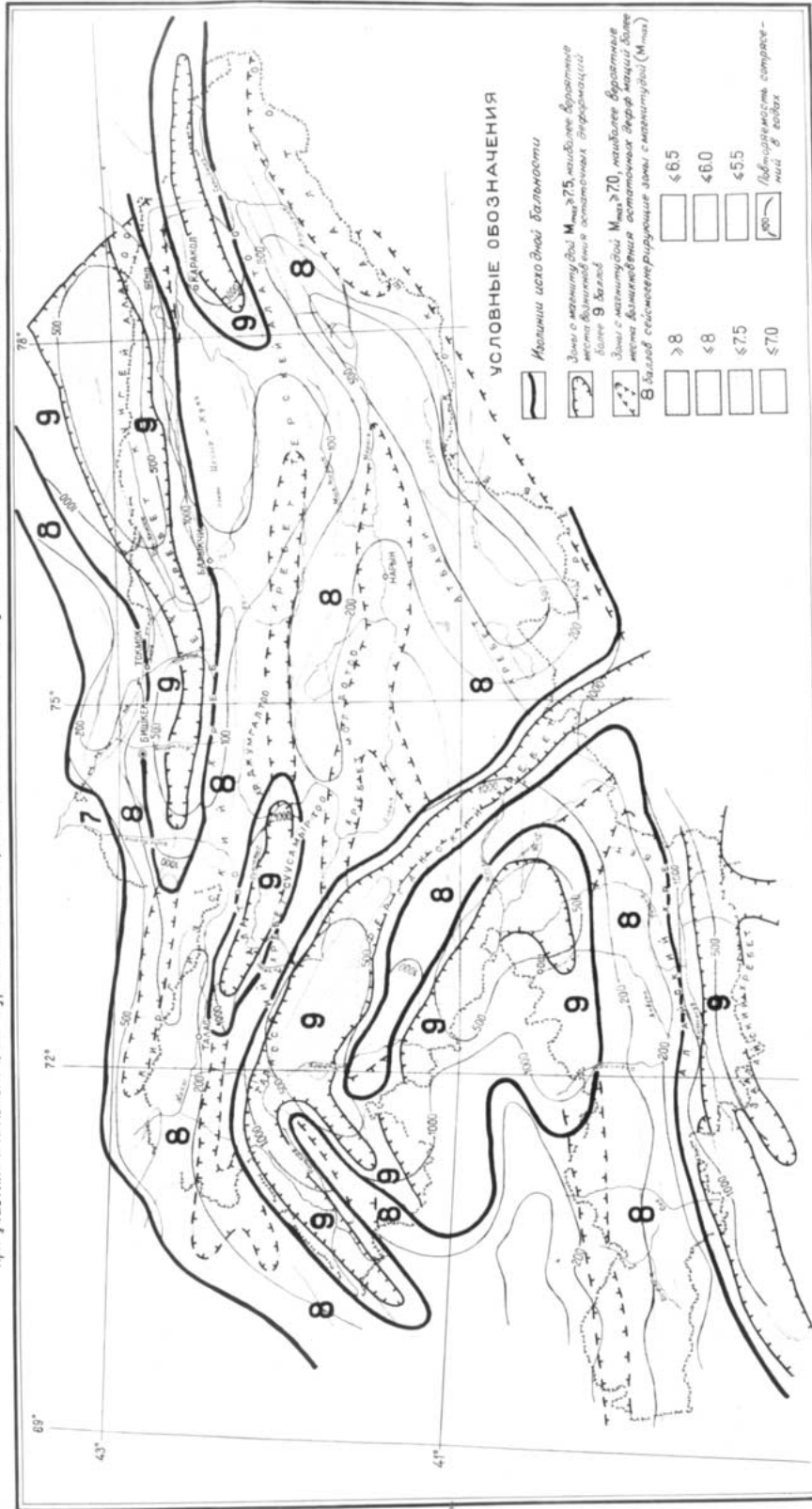


Figure 10. Seismic zonation map of Kyrgyzstan (Djanusakov et al., 1995). Seismic hazard zones are outlined by bold black lines and classified in terms of ballovs – intensities. Inside the 9-ballovs zones, hooked lines delimit areas with expected maximum magnitudes larger than 7.5. Inside the 8-ballovs zones, dashed-hooked lines delimit areas with expected maximum magnitudes larger than 7.0.

of 50 years with 90%-probability of non-exceedance. Site effects have not been taken into account in this study.

Acknowledgements

The research leading to this article was funded by the European Community (EC, DG XII contract IC15-CT97-0202) and by the Fonds National de la Recherche Scientifique, Belgium. We wish to thank D.M. Boore for allowing us to use the SMSIM program and A. Strom for constructive discussion.

References

- Abdrakhmatov, K.Ye, Aldazhanov, S.A., Hager, B.H., Hamburger, M.W., Herring, T.A., Kalabaev, K.B., Makarov, V.I., Molnar, P., Panasyuk, S.V., Prilepin, M.T., Reilinger, R.E., Sadybakasov, I.S., Souter, B.J., Trapeznikov, Yu.A., Tsurkov, V.Ye. and Zubovich, A.V., 1996, Relatively recent construction of the Tien Shan inferred from GPS measurements of present-day crustal deformation rates, *Nature* **384**, 450–453.
- Allen, M.B. and Vincent, S.J., 1999, Late Cenozoic tectonics of the Kippingtage thrust zone: Interactions of the Tien Shan and Tarim Basin, Northwest China, *Tectonics* **18**(4), 639–654.
- Ambraseys, N.N., K.A. Simpson and Bommer, J.J., 1996, Prediction of horizontal response spectra in Europe, *EESD* **25**, 371–400.
- Arias, A., 1970, A measure of earthquake intensity. In: Hansen, R.J. (ed.), *Seismic Design for Nuclear Powerplants*, MIT Press, Cambridge, Massachusetts, pp. 438–483.
- Atkinson, G.M. and Silva, W., 1997, An empirical study of Earthquake source spectra for California earthquakes, *Bull. Seis. Soc. Am.* **87**(1), 97–113.
- Atkinson, G.M. and Boore, D.M., 1995, Ground motion relations for Eastern North America, *Bull. Seis. Soc. Am.* **85**(1), 17–30.
- Bender, B. and Perkins, D.M., 1987, SEISRISKIII: A computer program for seismic hazard estimation, *U.S. Geol. Surv. Prof. Paper* **1772**.
- Bogdanovich, M.M.C., Kark, J., Korolkov, B. and Muchketov, D., 1914, Earthquake of the 4th January 1911 in the northern districts of the Tien Shan, *Tr. Geol. Com. Ser.* **89**, 270 p.
- Boore, D.M., 1996, SMSIM-Fortran programs for simulating ground motions from earthquakes: version 1.0, *U.S. Geol. Surv. Open-File Rept.* 96-80-A, 73 pp.
- Boore, D.M. and Joyner, W.B., 1997, Site amplifications for generic rock sites, *Bull. Seis. Soc. Am.* **87**(2), 327–341.
- Brune, J.N., 1970, Tectonic stress and the spectra of seismic shear waves from earthquakes, *J. Geoph. Res.* **75**(26), 4997–5009.
- Cobbold, P.R., Sadybakasov, E. and Thomas, J.C., 1994, Cenozoic transpression and Basin development, Kyrgyz Tien Shan, Central Asia. In: Roure, F., Ellouz, N., Shein, V.S. and Skvortsov, I. (eds.), *Geodynamics Evolution of Sedimentary Basins*, Technip, Paris, pp. 181–202.
- Delvaux, D., Abdrakhmatov, K.E. and Strom, A.L., 2001, Landslides and surface breaks of the Ms 8.2 Kemin earthquake, Kyrgyzstan, Russian Geology and Geophysics, *Geologiya i Geofizika* **42**(10), 1167–1177.
- Djanuzakov, K.D., Chedia, O.K., Abdrakhmatov, K.E. and Turdukulov, A.T., 1995, *Seismic Zonation Map of Kyrgyz Republic*, Bishkek, Ilim.
- Faccioli, E., 1995, Induced Hazards: Earthquake triggered Landslides. In: Proc. 5th Intern. Conf. on Seismic Zonation, Nice, France, Oct. 17–19, pp. 1–24.
- Fan, G., Ni, J.F. and Wallace, T.C., 1994, Active tectonics of the Pamirs and the Karakorum, *J. Geoph. Res.* **99**(B4), 7131–7160.
- Geological map of Kirghiz SSR, 1980, Akad. Nauk Kirghiz SSR and Ministry of Geology, USSR, scale: 1:200,000.
- Ghose, S., Mellors, R.J., Korjenkov, A.M., Hamburger, M.W., Pavlis, T.L., Pavlis, G.L., Mamyrov, E. and Muraliev, A.R., 1997, The Ms = 7.3 1992 Suusamy, Kyrgyzstan earthquake: 2. Aftershock Focal Mechanisms and Surface Deformation, *Bull. Seism. Soc. Am.* **87**(1), 23–38.
- Harp, E.L. and Wilson, R.C., 1995, Shaking intensity thresholds for rock falls and slides: evidence from 1987 Whittier Narrows and Superstition Hills earthquake strong-motion records, *Bull. Seis. Soc. Am.* **85**(6), 1739–1757.
- Havenith, H.-B., Jongmans, D., Faccioli, E., Abdrakhmatov, K and Bard, P.-Y., Site effect analysis around the seismically induced Ananevo rockslide Kyrgyzstan, *Bull. Seis. Soc. Am.*, in press.
- Huo, J. and Hu, Y., 1992, Study on attenuation laws of ground motion parameters, *Earth. Eng. Eng. Vibration* **12**, 1–11.
- Imanbekov, S., Dzhanuzov, K., Uranova, S. and Frolova, A., 1999, Seismic hazard and building vulnerability in Kyrgyzstan. In: King, S.A., Khalturin, V.I. and Tucker, B.E. (eds.), *Seismic Hazard and Building Vulnerability in Post-Soviet Central Asian Republics*, Kluwer Academic Publishers, Dordrecht, pp. 93–105.
- Jibson, R.W., Harp, E.L. and Michael, J.A., 1998, A method for producing digital probabilistic seismic landslide hazard maps: An example from Los Angeles, California, Area, *U.S. Geol. Surv. Open-file Report* 98-113, 23 pp.
- Joyner, W.B., 1984, A scaling law for the spectra of large earthquakes, *Bull. Seism. Soc. Am.* **74**, 1167–1188.
- Keefer, D.K. and Wilson, R.C., 1989, Predicting earthquake-induced landslides, with emphasis on arid and semi-arid environments. In: Sadler, P.M. and Morton, D.M. (eds.), *Landslides in a Semi-Arid Environment*, Inland Geological Society, **2**, pp. 118–149.
- Margaris, B.N. and Boore, D.M., 1998, Determination of and from response spectra of large earthquakes in Greece, *Bull. Seis. Soc. Am.* **88**(1), 170–182.
- Mellors, R.J., Vernon, F.L., Pavlis, G.L., Abers, G.A., Hamburger, M.W., Ghose, S. and Illiasov, B., 1997, The Ms = 7.3 1992 Suusamy, Kyrgyzstan earthquake: 1. Constraints on fault geometry and source parameters based on aftershocks and body wave modeling, *Bull. Seism. Soc. Am.* **87**, 11–22.
- Miles, S.B. and Ho, C.L., 1999, Rigorous landslide hazard zonation using Newmark's method and stochastic ground motion simulation, *Soil Dyn. Earth. Eng.* **18**, 305–323.
- Molnar, P. and Tapponier, P., 1975, Cenozoic Tectonics of Asia: Effects of a continental collision, *Science* **189**(4201), 419–426.
- Muraliev, A., Abdrakhmatov, K. and Kuchai, O., 2000, Final report on INCO-COPERNICUS PL 96-3202, Landslides triggered by earthquakes, Seismological part.
- Peng, K.Z., Wu, F.T. and Song, L., 1985, Attenuation characteristics of peak horizontal acceleration in Northeast and Southwest China, *EESD* **13**, 337–350.
- Reigber, C., Angermann, D., Michel, G.W., Klotz, J., Galas, R. and the CATS-team, 1997, New constraints on the distribution of deformation in Central Asia: GPS results covering the Tien Shan, N-Pamir and Tarim. In *Proc. of 24th General Assembly on Geophysical Research*, The Hague, **1**(1), p. 39.

- Ulomov, V.I. and the GSHAP Region 7 working group, 1999, Seismic hazard of Northern Eurasia, *Annali di Geofisica* **42**(6), 1023–1038.
- Wilson, R.C. and Keefer, D.K., 1985, Predicting the areal limits of earthquake-induced landsliding. In: Ziony, J.I. (ed.), *Evaluating Earthquake Hazards in the Los Angeles Region – An Earth Science Perspective*, U.S. Geol. Surv. Prof. Paper **1360**, pp. 316–345.
- Zhang, P., Yang, Z., Gupta, H.K., Bhatia, S.C. and Shedlock, K.M., 1999, Global seismic hazard assessment program (GSHAP) in continental Asia, *Annali di Geofisica* **42**(6), 1167–1190.

Annex

- Zone 1: The Talas Basin and Southern Karatau mountains.
- Zone 2: The Kyrgyz Range bordered in the North by several active faults (e.g. Chonkurchak (a) and Issyk-Ata (b) faults).
- Zone 3: The Chu Basin.
- Zone 4: The Kindl-Tas Range.
- Zone 5: Chon Kemin – Chilik zone composed of Zaili, Sugety and Kungei Ranges including seismically active faults, that produced events of $m > 8$: Chon Kemin-Chilik (strike-slip, a) and Chon Aksu (thrusting, b).
- Zone 6: Ketmen Range.

- Zone 7: Ugam mountains with Range bordering active faults.
- Zone 8: Chatkal Range with Range bordering active faults.
- Zone 9: Suusamyр region including Suusamyр Basin and Range. The $M_s = 7.3$ Suusamyр earthquake occurred on the Aramsu fault (a).
- Zone 10: Kochkor and Djumgal Basins.
- Zone 11: Issyk Kul Basin.
- Zone 12: Teskey Range with active PredTeskey (a) fault.
- Zone 13: Northern Fergana Basin.
- Zone 14: Central Fergana Basin.
- Zone 15: Southern Fergana Basin.
- Zone 16: Central Fergana Range with active Arslanbob fault (a).
- Zone 17: Naryn Basin.
- Zone 18: Atbashi Basin and Range.
- Zone 19: Saryaz Range.
- Zone 20: Alay and Turkesten Ranges including.
- Zone 21: Kokshal Range.
- Zone 22: Akesu Basin with western extension of seismically active Baicheng-Kuche thrust system (a).
- Zone 23: Alay Basin bordered in the North in the South by the seismically active Northern Pamir thrust (a).
- Zone 24: Kipintage thrust zone delimited in the South by the active Kipintage thrust fault (a) and including the active Piqiang (b) fault.